

Ghost dark energy in the DGP braneworld

M. Abdollahi Zadeh^{1*} and A. Sheykhi^{1,2†}

¹ *Physics Department and Biruni Observatory, College of Sciences, Shiraz University, Shiraz 71454, Iran*

² *Research Institute for Astronomy and Astrophysics of Maragha (RIAAAM), P.O. Box 55134-441, Maragha, Iran*

We investigate the ghost model of dark energy in the framework of DGP braneworld. We explore the cosmological consequences of this model by determining the equation of state parameter, ω_D , the deceleration and the density parameters. We also examine the stability of this model by studying the squared of the sound speed in the presence/absence of interaction term between dark energy and dark matter. We find out that in the absence of interaction between two dark sectors of the Universe we have $\omega_D \rightarrow -1$ in the late time, while in the presence of interaction ω_D can cross the phantom line -1 . In both cases the squared of sound speed v_s^2 does not show any signal of stability. We also determine the statefinder diagnosis of this model as well as the $\omega_D - \omega'_D$ plane and compare the results with the Λ CDM model. We find that $\omega_D - \omega'_D$ plane meets the freezing region in the absence of interaction between two dark sectors, while it meets both the thawing and the freezing regions in the interacting case.

I. INTRODUCTION

The current acceleration of the Universe expansion which was strongly confirmed by the type Ia supernova observations [1] and also supported by the astrophysical data obtained from WMAP [2], indicates the existence of a fluid with negative pressure, which can overcome the gravity force between the galaxies and push them to accelerate. It is a general belief that dark energy (DE) is responsible for such an acceleration, though its nature and origin is still an open question in the modern cosmology. There are two approaches for explanation of the cosmic acceleration. (i) the modified gravity models such as $f(R)$ gravity [3] and scalar-tensor theories [4], (ii) the idea of the existence of a strange type of energy whose gravity is repulsive such as the cosmological constant Λ [5] and the dynamical DE models [6, 7]. Against the cosmological constant Λ which has constant equation of state (EoS) parameter $\omega_D = -1$, the further observations detect a small variation in the EoS parameter of DE in favor of a dynamical DE with $\omega_D > -1$ in the past and even $\omega_D < -1$ in the late time [8].

An interesting model for probing the dynamical DE model is the ghost dark energy (GDE) model proposed in [9]. The advantages of this model is that it does not introduce any new degree of freedom in contrast to most DE models that explain the accelerated expansion by introduction new degree(s) of freedom or by modifying the underlying theory of gravity. This is important because, with introducing new degrees of freedom, one needs to investigate the nature and new consequences in the universe so it seems to be impressive and economic if we can explain DE puzzle by using currently known fluids and fields of nature. Actually, GDE model which is based on the Veneziano ghost in Quantum Chromodynamics (QCD) can act as the source of DE [10] and its existence are required for resolution of the U(1) problem in QCD [11]. Indeed, the ghosts are decoupled from the physical states and make no contribution in flat Minkowski space, but it produces a small vacuum energy density in a dynamic background or a curved spacetime proportional to $\Lambda_{QCD}^3 H$, where H is the Hubble parameter and Λ_{QCD} is QCD mass scale of order a $100 MeV$ [12]. Different features of GDE have been studied in ample details [13].

Independent of the DE puzzle, for explanation of the cosmic acceleration, special attention is also paid to extra dimensional theories, in which our Universe is realized as a 3-brane embedded in a higher dimensional spacetime. Based on the braneworld model, all the particle fields in the standard model are confined to a four-dimensional brane, while gravity is free to propagate in all dimension. One of the original model of braneworld is introduced by Dvali-Gabadadze-Porrati (DGP) [14], which describes our Universe as a 4D brane embedded in a 5D Minkowskian bulk with infinite size. In this model the recovery of the usual gravitational laws on the brane is obtained by adding an Einstein-Hilbert term to the action of the brane computed with the brane intrinsic curvature. It is a well known that the DGP model has two branches of solutions. The self-accelerating branch of DGP model can explain the late time cosmic speed-up without recourse to DE or other components of energy [15, 16]. However, the self-accelerating DGP branch has ghost instabilities and it cannot realize phantom divide crossing by itself. To realize phantom divide crossing it is necessary to add at least a component of energy on the brane. On the other hand, the normal DGP branch cannot explain acceleration but it has the potential to realize a phantom-like phase by dynamical screening

* m.abdollahizadeh@shirazu.ac.ir

† asheykhi@shirazu.ac.ir

on the brane. Adding a DE component to the normal branch solution brings new facilities to explain late time acceleration and also better matching with observations. These are the motivations to add DE to this braneworld setup [17, 18]. In this work we would like to investigate the GDE model in the framework of the DGP braneworld. This study is of great importance, since we can incorporate and disclose the effects of the extra dimension on the evolution of the cosmological parameters on the brane when the DE source is in the form of GDE.

This paper is organized as follow. In section II we formulate the GDE model in the context of the DGP braneworld. We also consider both interacting and noninteracting cases and explore various cosmological parameters as well as cosmological planes. Besides the discussion of instability analysis, we study the $\omega_D - \omega'_D$ plane and properties of statefinder parameters. We finish with closing remarks in section III.

II. THE GDE IN THE DGP MODEL

In the DGP cosmology, a homogeneous, spatially flat and isotropic 3-dimensional brane which is embedded in a 5-dimensional Minkowskian bulk, can be described by the following Friedmann equation [19]

$$H^2 = \left(\sqrt{\frac{\rho_m + \rho_D}{3m_p^2} + \frac{1}{4r_c^2}} + \frac{\epsilon}{2r_c} \right)^2, \quad (1)$$

or equivalently

$$H^2 - \frac{\epsilon}{r_c}H = \frac{1}{3m_p^2}(\rho_m + \rho_D), \quad (2)$$

where $H = \dot{a}/a$ is the Hubble parameter, $r_c = m_{\text{pl}}^2/(2m_5^3)$ [20] is the crossover length scale reflecting the competition between 4D and 5D effects of gravity and $\epsilon = \pm 1$ corresponds to the two branches of solutions of the DGP model. Before going any further, it is worthy to note that if $H^{-1} \ll r_c$ (early times) the 4D general relativity is recovered, otherwise the 5D effect becomes significant. Also $\epsilon = +1$ corresponds to the self-accelerating solution where the universe may accelerate in the late time purely due to modification of gravity [15, 16], while $\epsilon = -1$ can produce the acceleration only if a DE component is included on the brane. Here, to accommodate GDE into the formalism we take $\epsilon = -1$.

The fractional energy density parameters are defined as

$$\Omega_m = \frac{\rho_m}{3m_p^2 H^2}, \quad \Omega_D = \frac{\rho_D}{3m_p^2 H^2}, \quad \Omega_{r_c} = \frac{1}{4r_c^2 H_0^2}, \quad (3)$$

where H_0 is the Hubble parameter at redshift $z = 0$. The Friedmann equation (2) can be rewritten in terms Eq.(3) as

$$\Omega_m + \Omega_D + 2\epsilon \frac{H_0}{H} \sqrt{\Omega_{r_c}} = 1. \quad (4)$$

We introduce $\Omega_{DGP} = 2\epsilon \sqrt{\Omega_{r_c}} H_0/H$, which comes from the extra dimension. Thus the Friedmann equation (4) can be reexpressed as

$$\Omega_m + \Omega_D + \Omega_{DGP} = 1. \quad (5)$$

For the GDE density we have

$$\rho_D = \alpha H, \quad (6)$$

where α is a constant of order Λ_{QCD}^3 and Λ_{QCD} is the QCD mass scale [21]. Taking the time derivative of the energy density ρ_D and using Eq.(6) we obtain

$$\dot{\rho}_D = \rho_D \frac{\dot{H}}{H}. \quad (7)$$

For the FRW universe filled with DE and DM, with mutual interaction, the energy-momentum conservation law can be written as

$$\dot{\rho}_m + 3H\rho_m = Q, \quad (8)$$

$$\dot{\rho}_D + 3H(1 + \omega_D)\rho_D = -Q, \quad (9)$$

where $Q = 3b^2 H(\rho_D + \rho_m)$ is considered as the interaction term between DE and DM also b^2 is the coupling constant of interaction Q .

We know that (i) our Universe is in a DE dominated phase and (ii) our Universe that is our habitat is stable. These imply that any variable DE model should result a stable DE dominated universe. So it is worth investigating the stability of the GDE in DGP braneworld against perturbation. The intended indicator for checking the stability of a proposed DE model is to study the behavior of the squared sound speed ($v_s^2 = dP/d\rho$) [22]. If $v_s^2 < 0$ we have the classical instability of a given perturbation because the perturbation of the background energy density is an oscillatory function and may grow or decay with time. When $v_s^2 > 0$, we expect a stable universe against perturbations because the perturbation in the energy density, propagates in the environment. We continue discussion of stability in the linear perturbation regime where the perturbed energy density of the background can be written as

$$\rho(t, x) = \rho(t) + \delta\rho(t, x), \quad (10)$$

where $\rho(t)$ is unperturbed background energy density. For the energy conservation equation ($\nabla_\mu T^{\mu\nu} = 0$) which yields [22]

$$\delta\dot{\rho} = v_s^2 \nabla^2 \delta\rho(t, x), \quad (11)$$

we encounter two cases. In the first case where $v_s^2 > 0$, we observe an ordinary wave equation which have a wave solution in the form $\delta\rho = \delta\rho_0 e^{-i\omega t + i\vec{k}\cdot\vec{x}}$ (stable universe). In the second case where $v_s^2 < 0$, the frequency of the oscillations becomes pure imaginary and the density perturbations will grow with time as $\delta\rho = \delta\rho_0 e^{\omega t + i\vec{k}\cdot\vec{x}}$ (unstable universe). Since v_s^2 plays a crucial role in determining the stability of DE model, we rewrite it in terms of EoS parameter as

$$v_s^2 = \frac{\dot{P}}{\dot{\rho}} = \frac{\dot{\rho}_D w_D + \rho_D \dot{w}_D}{\dot{\rho}_D(1+u) + \rho_D \dot{u}}, \quad (12)$$

where $P = P_D$ is the pressure of DE, $\rho = \rho_m + \rho_D$ is the total energy density of DE and DM and $u = \Omega_m/\Omega_D$ is the energy density ration.

On the other sides, Sahni et al., [23] proposed new geometrical diagnostic pair parameter $\{r, s\}$, known as statefinder parameter, for checking the viability of newly introduced DE models. Unlike the physical variables which depend on the properties of physical fields describing DE models, the statefinder pair primarily depends on the scale factor and hence it depends on the metric of the spacetime. The r and s parameters are defined as [23]

$$r = \frac{\ddot{a}}{aH^3}, \quad s = \frac{r-1}{3(q-1/2)}, \quad (13)$$

where r can rewrite as

$$r = 1 + 3\frac{\dot{H}}{H^2} + \frac{\ddot{H}}{H^3}.$$

and then

$$r = 2q^2 + q - \frac{\dot{q}}{H}. \quad (14)$$

Let us note that in the $\{r, s\}$ plane, $s > 0$ corresponds to a quintessence-like model of DE and $s < 0$ corresponds to a phantom-like model of DE. Also the studies on a flat Λ CDM model and matter dominated universe (SCDM) show that for these models $\{r, s\} = \{1, 0\}$ and $\{r, s\} = \{1, 1\}$, respectively. In above equations q is the deceleration parameter which is given by

$$q = -1 - \frac{\dot{H}}{H^2}. \quad (15)$$

In what follows we discuss the $\omega_D - \omega'_D$ plane which introduced by Caldwell and Linder [24] for analyzing the dynamical property of various DE models and distinguish these models (ω'_D represents the evolution of ω_D). The models can be categorized into two different classes: (i) $\omega'_D > 0$ and $\omega_D < 0$ which present the thawing region. (ii) $\omega'_D < 0$ and $\omega_D < 0$ which present the freezing region. It should be noted that the Λ CDM model corresponds to a fixed point $\{\omega_D = -1, \omega'_D = 0\}$ in the $\omega_D - \omega'_D$ plane. We shall consider the noninteracting and interacting cases, separately.

A. Non interacting case

We start to obtain the cosmological parameters for GDE in the DGP braneworld by ignoring the interaction term ($Q = 0$). The deceleration parameter q can be obtained by taking the time derivative of Eq.(2), which lead to

$$\frac{\dot{H}}{H^2} = \frac{-3(1 - \Omega_{DGP}) + 3\Omega_D}{2 - \Omega_{DGP} - \Omega_D}. \quad (16)$$

Using relation (15), we find

$$q = -1 - \frac{-3(1 - \Omega_{DGP}) + 3\Omega_D}{2 - \Omega_{DGP} - \Omega_D}. \quad (17)$$

Inserting Eq. (7) in Eq. (9) we have

$$\omega_D = -1 - \frac{1}{3} \frac{\dot{H}}{H^2}, \quad (18)$$

where by replacing Eq.(16) in it, we get

$$\omega_D = -\frac{1}{2 - \Omega_{DGP} - \Omega_D}. \quad (19)$$

Also we obtain ω'_D from the above equation as

$$\omega'_D = -\frac{3(-1 + \Omega_{DGP} + \Omega_D)(\Omega_{DGP} + \Omega_D)}{(-2 + \Omega_{DGP} + \Omega_D)^3}. \quad (20)$$

Note that in order to find the evolution of density parameter Ω_D , we take the time derivative of relation $\Omega_D = \rho_D/(3m_p^2 H^2)$, after combining the result with Eqs .(7) and (16), yields

$$\Omega'_D = \Omega_D(1 + q). \quad (21)$$

In Fig. 1, we plot the evolution of Ω_D versus redshift parameter z . It is obvious that Ω_D tends to 0 in the early

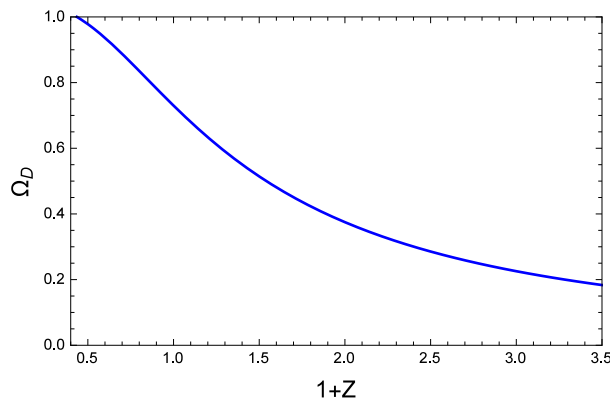


FIG. 1: The evolution of Ω_D versus redshift parameter z for noninteracting GDE in DGP model . Here, we have taken $\Omega_D(z = 0) = 0.73$, $H(z = 0) = 67$ and $\Omega_{r_c} = 0.0003$

universe where $1 + z \rightarrow \infty$, while at the late time where $1 + z \rightarrow 0$, we have $\Omega_D \rightarrow 1$. Clearly, Eq.(19) for the EoS parameter shows that at the late time where $\Omega_D \rightarrow 1$, the EoS parameter mimics the cosmological constant, namely $\omega_D \rightarrow -1$. In Fig. 3, the behavior of the deceleration parameter q is plotted and indicates that indeed there is a decelerated expansion at the early stage of the universe followed by an accelerated expansion. The energy density ratio is defined as $u = \Omega_m/\Omega_D$, which by using Eq.(5) can be written

$$u = -1 + \frac{1}{\Omega_D}(1 - \Omega_{DGP}). \quad (22)$$

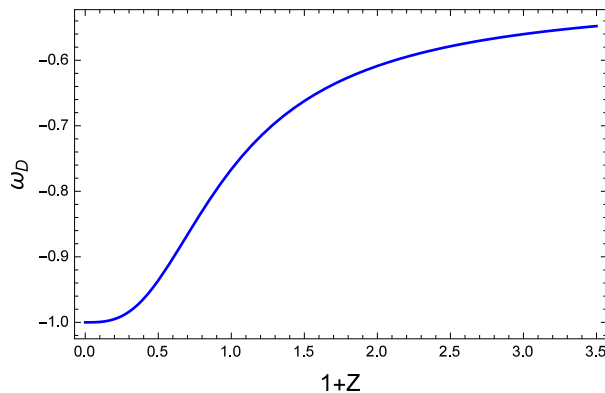


FIG. 2: The evolution of ω_D versus redshift parameter z for noninteracting GDE in DGP model . Here, we have taken $\Omega_D(z=0) = 0.73$, $H(z=0) = 67$ and $\Omega_{r_c} = 0.0003$

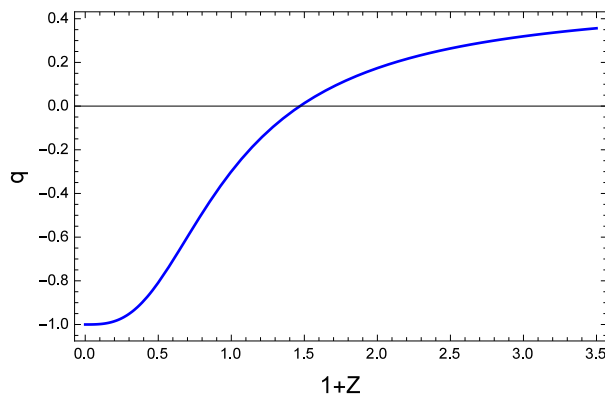


FIG. 3: The evolution of the deceleration parameter q versus redshift parameter z for noninteracting GDE in DGP model . Here, we have taken $\Omega_D(z=0) = 0.73$, $H(z=0) = 67$ and $\Omega_{r_c} = 0.0003$

Differentiating Eqs. (22) and (19) and then substituting the results in Eq. (12) we get the squared of sound speed as

$$v_s^2 = -\frac{2\Omega_D(-1 + \Omega_{DGP} + \Omega_D)}{(-2 + \Omega_{DGP})(-2 + \Omega_{DGP} + \Omega_D)^2}. \quad (23)$$

The evolution of v_s^2 against z for the noninteracting GDE in the framework of DGP braneworld is plotted in Fig. 4. From graphical analysis of v_s^2 one concludes that this model does not indicate any signal of stability, that is $v_s^2 < 0$ during the history of the universe. We can also find the statefinder parameters r and s by taking derivative of Eq.(17) and using Eq.(13) and Eq.(14). The results are

$$r = 10 + \frac{18}{(-2 + \Omega_{DGP} + \Omega_D)^3} + \frac{45}{(-2 + \Omega_{DGP} + \Omega_D)^2} + \frac{36}{-2 + \Omega_{DGP} + \Omega_D}, \quad (24)$$

$$s = \frac{2(-1 + \Omega_{DGP} + \Omega_D)^2}{(-2 + \Omega_{DGP} + \Omega_D)^2}. \quad (25)$$

The graphical behavior of the statefinder parameters $\{r, s\}$ given in Eqs. (24) and (25), are plotted in Figs. 5 and 6, showing that at late time where $\Omega_D \rightarrow 1$, we have $\{r, s\} = \{1, 0\}$ which implies that GDE mimics the cosmological constant at the late time, as expected.

Let us study the trajectory in the statefinder plane and analyze this model from the statefinder viewpoint. For this purpose, we plot the statefinder diagram in the $r - s$ in Fig. 7, which shows the curve gets to the point $\{r, s\} = \{1, 0\}$ in the end, which implies that the model corresponds to the Λ CDM model at the late time. For complementarity of the diagnostic, we also plot the trajectories of statefinder pair $r - q$ in Fig. 8 which ends in the future to $r = 1$, $q = -1$ corresponding to the de-Sitter expansion.

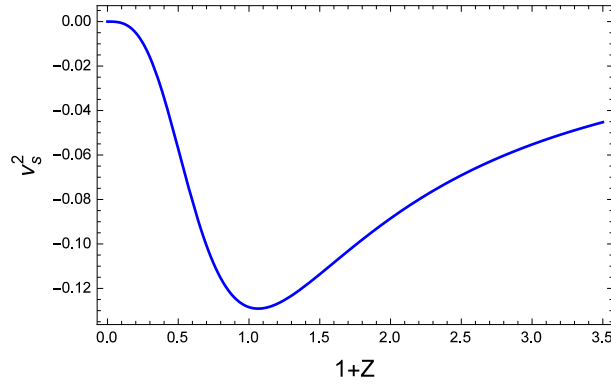


FIG. 4: The evolution of the squared of sound speed v_s^2 versus redshift parameter z for noninteracting GDE in DGP model. Here, we have taken $\Omega_D(z=0) = 0.73$, $H(z=0) = 67$ and $\Omega_{r_c} = 0.0003$.

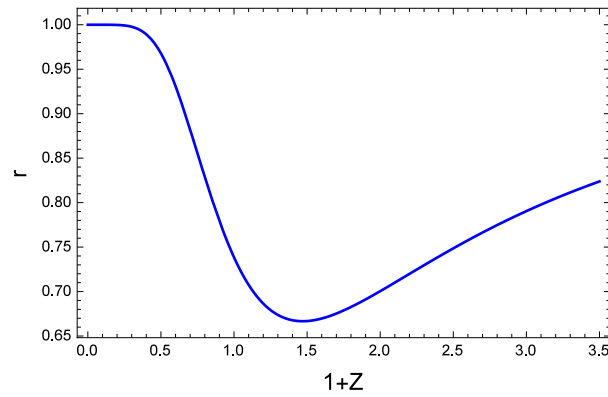


FIG. 5: The evolution of the statefinder parameter r versus the redshift parameter z for noninteracting GDE in DGP model. Here, we have taken $\Omega_D(z=0) = 0.73$, $H(z=0) = 67$ and $\Omega_{r_c} = 0.0003$.

The $\omega_D - \omega'_D$ plane for the noninteracting GDE in the DGP scenario is shown in Fig. 9. Again, we see that this plane corresponds to Λ CDM model, i. e., $(\omega_D = -1, \omega'_D = 0)$ and the trajectory meets the freezing region as well.

B. Interacting case

Differentiating the modified Friedmann equation (2) and using Eqs.(7) and (8) we reach

$$\frac{\dot{H}}{H^2} = \frac{3(b^2 - 1)(1 - \Omega_{DGP}) + 3\Omega_D}{2 - \Omega_{DGP} - \Omega_D}, \quad (26)$$

$$q = -1 - \frac{3(b^2 - 1)(1 - \Omega_{DGP}) + 3\Omega_D}{2 - \Omega_{DGP} - \Omega_D}. \quad (27)$$

Next, the EoS parameter can be determined by substituting Eq.(7) in the semi-conservation law Eq.(9) and using Eq.(26). We find

$$\omega_D = \frac{b^2(\Omega_{DGP} - 2)(\Omega_{DGP} - 1) + \Omega_D}{\Omega_D(-2 + \Omega_{DGP} + \Omega_D)}. \quad (28)$$

Taking differentiation with respect to $x = \ln a$ from above equation we get

$$\omega'_D = -\frac{3[(-1 + b^2)(-1 + \Omega_{DGP}) - \Omega_D][b^2(-2 + \Omega_{DGP})^2 + (-\Omega_{DGP} + b^2(-4 + 3\Omega_{DGP}) - \Omega_D)\Omega_D]}{\Omega_D(-2 + \Omega_{DGP} + \Omega_D)^3}, \quad (29)$$

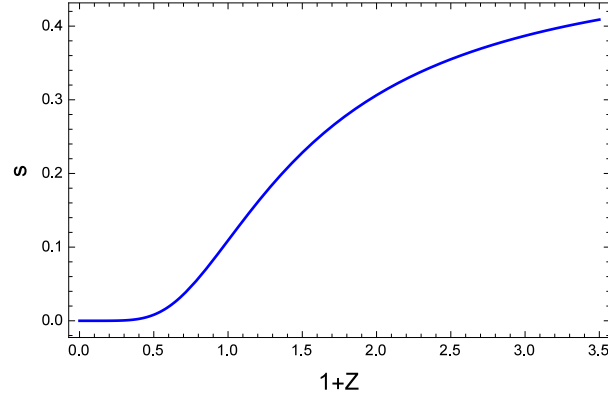


FIG. 6: The evolution of the statefinder parameter s versus the redshift parameter z for noninteracting GDE in DGP model . Here, we have taken $\Omega_D(z=0) = 0.73$, $H(z=0) = 67$ and $\Omega_{r_c} = 0.0003$.

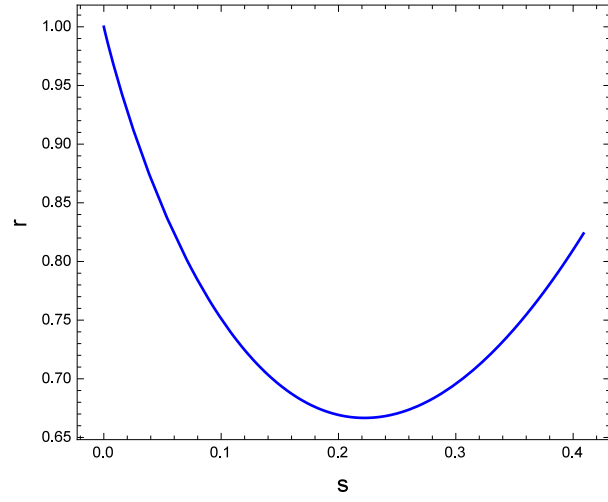


FIG. 7: The evolution of the statefinder parameter r versus s for noninteracting GDE in the DGP model . Here, we have taken $\Omega_D(z=0) = 0.73$, $H(z=0) = 67$ and $\Omega_{r_c} = 0.0003$.

where the prime indicates derivative with respect to $x = \ln a$. We can obtain the equation of motion for Ω_D as

$$\Omega'_D = \frac{3\Omega_D(-1 + \Omega_D + \Omega_{DGP} + b^2(1 - \Omega_{DGP}))}{-2 + \Omega_{DGP} + \Omega_D}, \quad (30)$$

To illustrate the cosmological consequences of the interacting GDE in the DGP braneworld, we plot their evolution in terms of redshift parameter z . In Fig. 10, we present the graphical of Ω_D versus z for the different values of the coupling constant b^2 . As expected, we see both $\Omega_D \rightarrow 1$ and $\Omega_D \rightarrow 0$ for late time and early time, respectively. The graphical behavior of the EoS parameter for the different values of b^2 shows crossing of phantom line as plotted in Fig. 11. The stability of interacting GDE in DGP model can obtain by differentiating with respect time of Eqs.(22) and (28)

$$v_s^2 = -\frac{b^2[(-2 + \Omega_{DGP})^3 + \Omega_D(6 + (-6 + \Omega_{DGP})\Omega_{DGP})] + \Omega_D(-2 + 2\Omega_{DGP} + 2\Omega_D)}{(-2 + \Omega_{DGP})(-2 + \Omega_{DGP} + \Omega_D)^2}. \quad (31)$$

The evolution of the deceleration parameter q and the squared of sound speed v_s^2 versus redshift parameter z are plotted in Figs. 12 and 13 respectively. In Fig. 12, we see for different values of b^2 with the interacting GDE in DGP model, our universe has a phase transition from deceleration to an acceleration, while by keeping the same situation in Fig. 13, this universe cannot be stable. As the value of b^2 decreases the severity of instability also decreases. Like

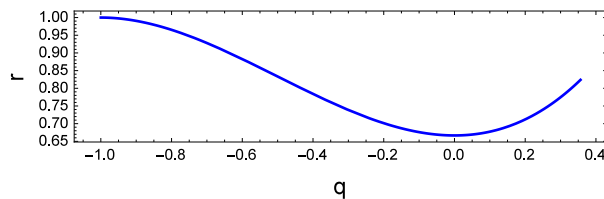


FIG. 8: The evolution of the statefinder parameter r versus the deceleration parameter q for noninteracting GDE in the DGP model . Here, we have taken $\Omega_D(z = 0) = 0.73$, $H(z = 0) = 67$ and $\Omega_{r_c} = 0.0003$.

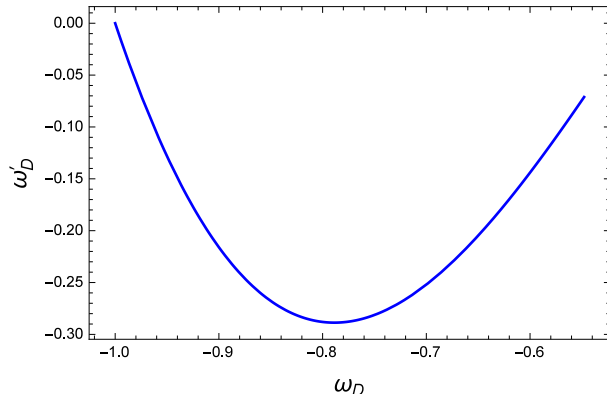


FIG. 9: The $\omega_D - \omega'_D$ diagram for noninteracting GDE in the DGP model . Here, we have taken $\Omega_D(z = 0) = 0.73$, $H(z = 0) = 67$ and $\Omega_{r_c} = 0.0003$.

previous section, the statefinder parameters obtain by taking derivative of Eq.(27) and using Eq.(13) and Eq.(14)

$$r = 10 + \frac{18(1 + b^2 - b^2\Omega_{DGP})}{(-2 + \Omega_{DGP} + \Omega_D)^3} + \frac{9(-1 + b^2(-1 + \Omega_{DGP}))(-5 + b^2(-3 + 2\Omega_{DGP}))}{(-2 + \Omega_{DGP} + \Omega_D)^2} + \frac{9(4 + b^2(4 - 3\Omega_{DGP}))}{-2 + \Omega_{DGP} + \Omega_D}, \quad (32)$$

$$s = 2 + \frac{2 - 2b^2(-1 + \Omega_{DGP})}{(-2 + \Omega_{DGP} + \Omega_D)^2} + \frac{4 + b^2(3 - 2\Omega_{DGP})}{-2 + \Omega_{DGP} + \Omega_D} + \frac{b^2}{2b^2(1 - \Omega_{DGP}) + \Omega_{DGP} + \Omega_D}. \quad (33)$$

We obtain $\{r, s\} = \{1, 0\}$ for Λ CDM model from Eqs.(32) and (33) in the limiting case where $b^2 = 0$, $\Omega_{DGP} = 0$ and $\Omega_D \rightarrow 1$ (in the late time). Also, Figs. 14 and 15 show that r and s are positive through the entire life of the Universe and turn to 1 and 0 at the late time, respectively. The $\{r, s\}$ evolutionary trajectories for the interacting GDE in the framework of the DGP braneworld for different values of b^2 are shown in Fig. 16. From Fig. 16, we can see that at the late time all curves tend to the Λ CDM fixed point $\{r = 1, s = 0\}$, also different b^2 , results in different evolution trajectories of statefinder which states r is smaller when b^2 is larger. The $r - q$ diagrams are plotted for different values of b^2 in Fig. 17 which mimics the de Sitter expansion, namely $r = 1$, $q = -1$ in the far future where $z \rightarrow 0$. In Fig. 18, we plot the $\omega_D - \omega'_D$ plane for different values of b^2 which show the trajectories meet both the thawing and the freezing regions as well.

III. CLOSING REMARKS

We have made a versatile study on both noninteracting and interacting GDE in the framework DGP model through well-known cosmological parameters as well as planes. We summarize our results as follows. For noninteracting case, we have found that the density parameter tends to zero at the early universe while at the late time we have $\Omega_D \rightarrow 1$. Meanwhile the EoS parameter cannot cross the phantom line and mimics the cosmological constant at the late time (Fig. 2). We have shown in that our Universe has a phase transition from deceleration to an acceleration, though we do not receive any signal of stability. The statefinder plane shows the trajectory corresponds to quintessence model

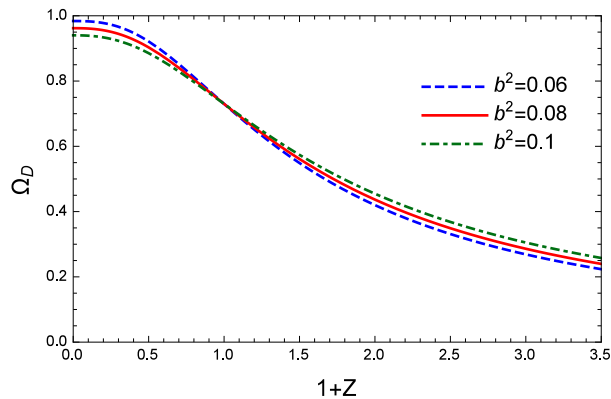


FIG. 10: The evolution of Ω_D versus redshift parameter z for interacting GDE in the DGP model. Here, we have taken $\Omega_D(z=0) = 0.73$, $H(z=0) = 67$ and $\Omega_{r_c} = 0.0003$

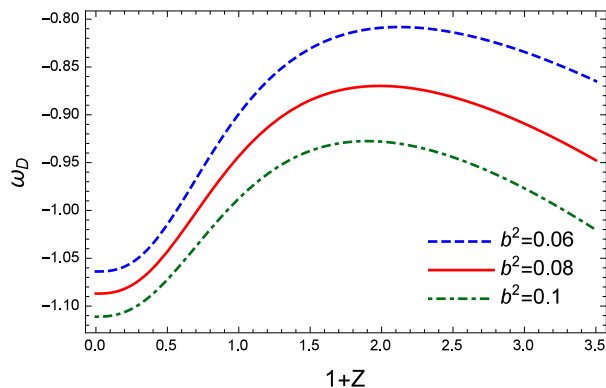


FIG. 11: The evolution of ω_D versus redshift parameter z for interacting GDE in the DGP model. Here, we have taken $\Omega_D(z=0) = 0.73$, $H(z=0) = 67$ and $\Omega_{r_c} = .0003$.

($s > 0$ and $r < 1$) while at late time we have $\{r, s\} = \{1, 0\}$ for Λ CDM model as expected. The $\omega_D - \omega'_D$ plane in Fig. 9 meets the freezing region as well.

For interacting case, we find that the density and the deceleration parameters as well as the EoS parameter are consistent with observational data. We have seen that as the value of b^2 decreases the severity of instability decreases. From $r - s$ plane, we can see that at the late time all curves tend to the Λ CDM fixed point $\{r = 1, s = 0\}$. Besides, for different values of b^2 , the different evolution trajectories of statefinder are shown which indicates that r is smaller when b^2 is larger. The $r - q$ plane is plotted in Fig. 17 which mimics the de Sitter expansion, namely $r = 1, q = -1$ in the far future where $z \rightarrow 0$. In the end, the $\omega_D - \omega'_D$ plane exhibits both freezing and thawing regions of the universe for all values of b^2 . Again, in this case $v_s^2 < 0$ which implies that interacting GDE in the DGP braneworld is not stable against perturbation.

Acknowledgments

We thank Shiraz University Research Council. This work has been supported financially by Research Institute for Astronomy & Astrophysics of Maragha (RIAAM), Iran.

[1] S. Perlmutter et al., *Astrophys. J.* **517**, 565 (1999);
P.M. Garnavich et al., *Astrophys. J.* **493**, L53 (1998);

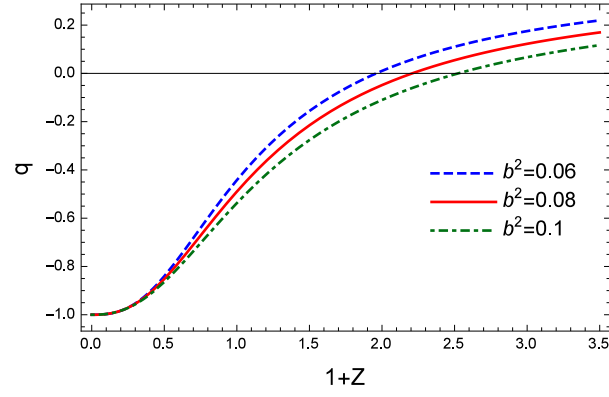


FIG. 12: The evolution of the deceleration parameter q versus redshift parameter z for interacting GDE in the DGP model . Here, we have taken $\Omega_D(z = 0) = 0.73$, $H(z = 0) = 67$ and $\Omega_{r_c} = 0.0003$.

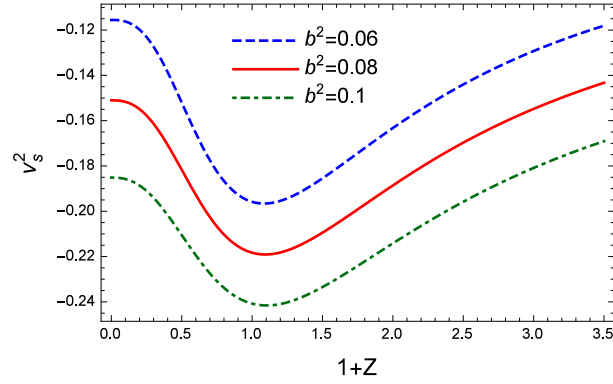


FIG. 13: The evolution of the squared of sound speed v_s^2 versus redshift parameter z for interacting GDE in the DGP model . Here, we have taken $\Omega_D(z = 0) = 0.73$, $H(z = 0) = 67$ and $\Omega_{r_c} = 0.0003$

- A.G. Riess et al., *Astron. J.* **116**, 1009 (1998);
D.N. Spergel et al., *Astrophys. J. Suppl.* **148**, 175 (2003);
A.G. Riess, *Astrophys. J.* **607**, 665 (2004);
P.J. Peebles, B. Ratra, *Rev. Mod. Phys.* **75**, 559 (2003).
[2] G.F. Hinshaw et al. *ApJS* **208**, 19 (2013).
[3] S. Capozziello, V. F. Cardone, S. Carloni and A. Troisi, *Int. J. Mod. Phys. D* **12**, 1969 (2003);
S. M. Carroll, V. Duvvuri, M. Trodden and M. S. Turner, *Phys. Rev. D* **70**, 043528 (2004);
S. Nojiri, S.D. Odintsov, *Int. J. Geom. Meth. Mod. Phys.* **4**, 115 (2007);
M. Sadegh Movahed, S. Baghran and S. Rahvar, *Phys. Rev. D* **76**, 044008 (2007);
S. Baghran, M. Sadegh Movahed and S. Rahvar, *Phys. Rev. D* **80**, 064003 (2009);
T.P. Sotiriou and V. Faraoni *Rev. Mod. Phys.* **82**, 451 (2010);
S. Nojiri and S.D. Odintsov, *Phys. Rep.* **505**, 59 (2011);
M. Tegmark et al., *Astrophys. J.* **606**, 702 (2004);
M. Kowalski et al., *Astrophys. J.* **686**, 749 (2008);
E. Komatsu et al., *Astrophys. J. Suppl. Ser.* **180**, 330 (2009);
P. A. R. Ade et al., (Planck Collaboration), *Astron. Astroph.* **594**, A13 (2016);
G. Papagiannopoulos, S. Basilakos, J. D. Barrow, A. Paliathanasis, *Phys. Rev. D* **97**, 024026 (2018)
[4] L. Amendola, *Phys. Rev. D* **60**, 043501 (1999);
J. P. Uzan, *Phys. Rev. D* **59**, 123510 (1999);
T. Chiba, *Phys. Rev. D* **60**, 083508 (1999);
N. Bartolo and M. Pietroni, *Phys. Rev. D* **61**, 023518 (2000);
V. Faraoni, *Cosmology in Scalar-Tensor Gravity*, Kluwer, Boston, (2004);
E. Elizalde, S. Nojiri, S. D. Odintsov, P. Wang, *Phys. Rev. D* **71**, 103504 (2005);
S. Nojiri, S. D. Odintsov, *Gen. Relativ. Gravit.* **38**, 1285 (2006) ;

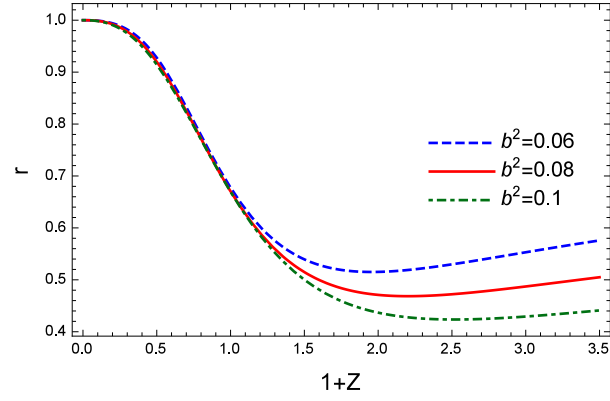


FIG. 14: The evolution of the statefinder parameter r versus the redshift parameter z for interacting GDE in DGP model . Here, we have taken $\Omega_D(z=0) = 0.73$, $H(z=0) = 67$ and $\Omega_{r_c} = .0003$.

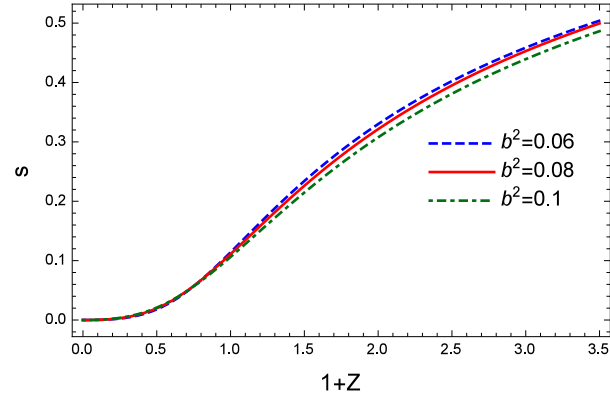


FIG. 15: The evolution of the statefinder parameter s versus the redshift parameter z for interacting GDE in the DGP model . Here, we have taken $\Omega_D(z=0) = 0.73$, $H(z=0) = 67$ and $\Omega_{r_c} = .0003$.

- R. Gannouji, et al., JCAP **0609**, 016 (2006);
 N. Banerjee, D. Pavon, Phys. Lett. B **647**, 447 (2007);
 A. Sheykhi, Phys. Lett. B **681**, 205 (2009);
 A. Sheykhi, Phys. Rev. D **81**, 023525 (2010);
 A. Sheykhi, M. Jamil, Phys. Lett. B **694**, 284 (2011);
 E. Ebrahimi, A. Sheykhi, Phys. Lett. B **706**, 19 (2011);
 A. Sheykhi, E. Ebrahimi, and Y. Yousefi, Can. J. Phys. **91**, 662 (2013);
 K. Karami, A. Sheykhi, M. Jamil, Z. Azarmi, M. M. Soltanzadeh, Gen. Relativ. Grav. **43**, 27 (2011);
 A. Pasqua, S. Chattopadhyay, Astrophys. Space Sci. **348**, 284 (2013);
 V. Fayaz, Astrophys. Space Sci. **361**, 86 (2016);
 P. Kumar, C.P. Singh, Astrophys. Space Sci. **362**, 52 (2017);
 Singh, C.P. Kumar, P. Int J Theor Phys **56**, 3297 (2017) ;
 F. Felegary, F. Darabi, M. R. Setare, Int. J. Mod. Phys. D. **27**, 1850017 (2018).
 [5] V. Sahni and A. Starobinsky, Int. J. Mod. Phys. D **9**, 373 (2000).
 [6] M. Li, Phys. Lett. B **603**, 1 (2004);
 S. D. H. Hsu, Phys. Lett. B **594**, 13 (2004);
 D. Pavon, W. Zimdahl, Phys. Lett. B **628**, 206 (2005) ;
 B. Guberina, R. Horvat, H. Stefancic, JCAP **0505**, 001 (2005);
 B. Guberina, R. Horvat, H. Nikolic, Phys. Lett. B **636**, 80 (2006);
 H. Li, Z. K. Guo, Y. Z. Zhang, Int. J. Mod. Phys. D **15**, 869 (2006) ;
 Q. G. Huang, Y. Gong, JCAP **0408**, 006 (2004) ;
 J. P. B. Almeida, J. G. Pereira, Phys. Lett. B **636**, 75 (2006) ;
 Y. Gong, Phys. Rev. D **70**, 064029 (2004) ;
 B. Wang, E. Abdalla, R. K. Su, Phys. Lett. B **611**, 21 (2005) ;

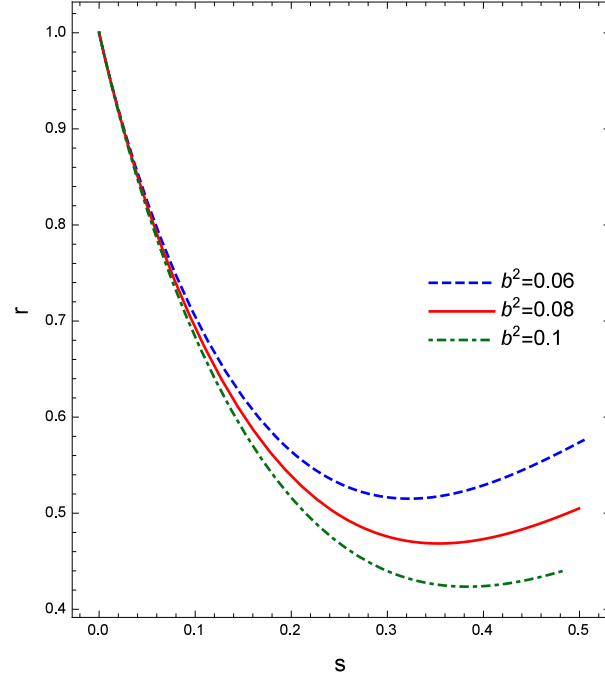


FIG. 16: The evolution of the statefinder parameter r versus s for interacting GDE in the DGP model. Here, we have taken $\Omega_D(z=0) = 0.73$, $H(z=0) = 67$ and $\Omega_{r_c} = .0003$.

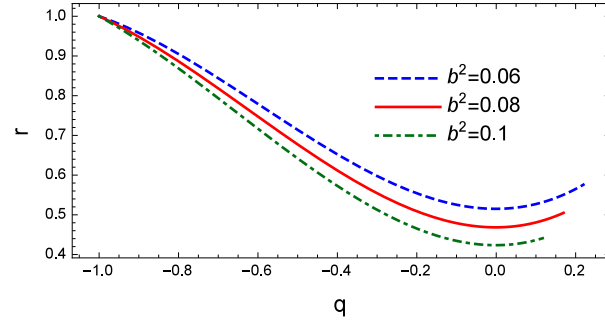


FIG. 17: The evolution of the statefinder parameter r versus the deceleration parameter q for interacting GDE in the DGP model. Here, we have taken $\Omega_D(z=0) = 0.73$, $H(z=0) = 67$ and $\Omega_{r_c} = .0003$.

- M. R. Setare, S. Shafei, JCAP **09**, 011 (2006) ;
M. R. Setare, Eur. Phys. J. C **50**, 991 (2007) ;
M. R. Setare, JCAP **0701**,023 (2007) ;
M. R. Setare, Phys. Lett. B **654**, 1 (2007);
M. R. Setare, E. C. Vagenas, Phys. Lett. B **666**, 111 (2008) ;
M. R. Setare, E. N. Saridakis, Phys. Lett. B **671**, 331 (2009) ;
C. Wetterich, Nucl. Phys. B **302**, 668 (1988);
B. Ratra and J. Peebles, Phys. Rev. D **37**, 3406 (1988);
R. R. Caldwell, Phys. Lett. B **545**23 (2002);
R. R. Caldwell, M. Kamionkowski and N. N. Weinberg, Phys. Rev. Lett. **91**, 071301 (2003);
Shin'ichi Nojiri, Sergei D. Odintsov, Phys.Lett. B **562**, 147 (2003);
T. Chiba, T. Okabe, and M. Yamaguchi, Phys. Rev. D **62**, 023511 (2000);
C. Armendariz-Picon, V. F. Mukhanov and P. J. Steinhardt, Phys. Rev. Lett. **85**, 4438 (2000);
C. Armendariz-Picon, V. F. Mukhanov and P. J. Steinhardt, Phys. Rev. D **63**, 103510 (2001);
A. Y. Kamenshchik, U. Moschella and V. Pasquier, Phys. Lett. B **511**265 (2001);
M. C. Bento, O. Bertolami, and A. A. Sen, Generalized Chaplygin Gas, Phys. Rev. D **66**, 043507 (2002);

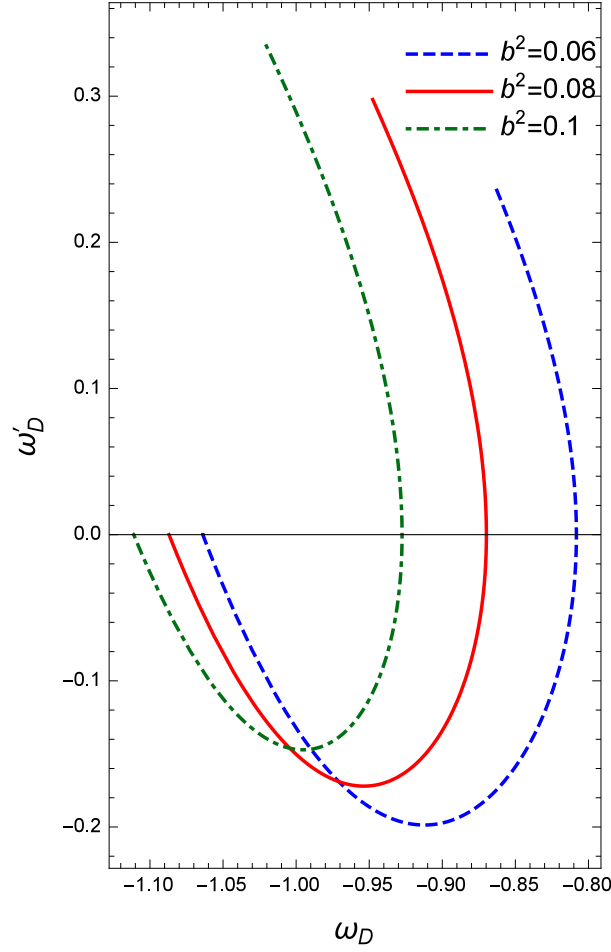


FIG. 18: The $\omega_D - \omega'_D$ diagram for interacting GDE in the DGP model. Here, we have taken $\Omega_D(z=0) = 0.73$, $H(z=0) = 67$ and $\Omega_{r_c} = .0003$.

- A. Sheykhi, *Class. Quantum Gravit.* **27**, 025007 (2010)
- [7] Shin'ichi Nojiri, Sergei D. Odintsov, *Gen.Rel.Grav.* **38**, 1285 (2006);
R. G. Cai, *Phys. Lett. B* **657**, 228 (2007);
H. Wei and R. G. Cai, *Phys. Lett. B* **660**, 113 (2008);
H. Wei and R. G. Cai, *Phys. Lett. B* **663**, 1 (2008);
J. P. Wu, D. Z. Ma, and Y. Ling, *Phys. Lett. B* **663**, 152 (2008);
J. Zhang, X. Zhang, and H. Liu, *Eur. Phys. J. C* **54**, 303 (2008);
A. Sheykhi, *Phys. Lett. B* **680**, 113 (2009);
A. Sheykhi, *Phys. Lett. B* **682**, 329 (2010);
I. Duran, L. Parisi, *Phys. Rev. D* **85**, 123538 (2012);
F. Yu, Jing-Fei Zhang, *Theor. Phys.* **59**, 243 (2013) 243;
P. Pankunni, Titus K. MATHEW, *Int. J. Mod. Phys. D* **23**, 1450024 (2014);
Y. Hu, M. Li, N. Li, Z. Zhang, *JCAP* **08**, 012 (2015);
HL. Li, JF. Zhang, L.Feng et al. *Eur. Phys. J. C* **77**, 907 (2017);
Ze. Zhao, Shuang. Wang, *Sci.China Phys.Mech.Astron.* **61**,039811 (2018);
A. Al Mamon, *Int. J. Mod. Phys. D* **26**, 1750136 (2017);
Sh. Wang, Yi. Wang, M. Li, *Physics Reports* **696**,1 (2017);
M. Abdollahi Zadeh, A. Sheykhi, H. Moradpour, *Int. J. Mod. Phys. D* **26**, 8 (2017).
- [8] B. Feng, X. L. Wang and X. M. Zhang, *Phys. Lett. B* **607**, 35 (2005);
U. Alam, V. Sahni and A. A. Starobinsky, *JCAP* **0406**, 008 (2004);
D. Huterer and A. Cooray, *Phys. Rev. D* **71**, 023506 (2005).
- [9] F. R. Urban and A. R. Zhitnitsky, *Phys. Lett. B* **688**, 9 (2010);
Phys. Rev. D **80**, 063001 (2009);

- JCAP **0909**, 018 (2009);
 Nucl. Phys. B **835**, 135 (2010).
- [10] G. Veneziano, Nucl. Phys. B **159**, 213 (1979).
- [11] E. Witten, Nucl. Phys. B **156**, 269 (1979);
 C. Rosenzweig, J. Schechter, C.G. Trahern, Phys. Rev. D **21**, 3388 (1980).
- [12] N. Ohta, Phys. Lett. B **695**, 41 (2011).
- [13] A. Sheykhi, M. Sadegh Movahed, Gen. Relativ. Gravit. **44**, 449 (2012);
 A. Sheykhi, A. Bagheri, Europhys. Lett. **95**, 39001 (2011);
 E. Ebrahimi, A. Sheykhi, Int. J. Mod. Phys. D, Vol. **20**, No. 12 2369 (2011);
 E. Ebrahimi, A. Sheykhi, H. Alavirad, Cent. Eur. J. Phys. Vol **11**, No.7, 949 (2013).
 C.-J. Feng, X.-Z. Li, P. Xi, JHEP **1205**, 046 (2012);
 C. J. Feng, X.-Z. Li, X.-Y. Shen, Phys. Rev. D **87**, 023006 (2013);
 C.-J. Feng, X.-Z. Li, X.-Y. Shen, Mod. Phys. Lett. A **27**, 1250182 (2012);
 S. Nojiri, S.D. Odintsov, Phys. Rev. D **72**, 023003 (2005);
 S. Capozziello, V.F. Cardone, E. Elizalde, S. Nojiri, S.D. Odintsov, Phys. Rev. D **73**, 043512 (2006);
 M.Z. Khurshudyan, A.N. Makarenko, Astrophys Space Sci **361** 187.(2016);
 M. Malekjani, T. Naderi, F. Pace, MNRAS **453**, 4148 (2015);
 E. Ebrahimi, H. Golchin, A. Mehrabi, S. M. S. Movahed IJMPD, **26**,1750124 (2017);
 M. Abdollahi Zadeh, A. Sheykhi, H. Moradpour, Int. J. Theor. Phys. **56**, 3477 (2017).
- [14] G.R. Dvali, G. Gabadadze, M. Porrati, Phys. Lett. B **485** 208 (2000).
- [15] C. Deffayet, Phys. Lett. B **502**, 199 (2001).
- [16] C. Deffayet and G. Dvali, Phys. Rev. D **65**, 044023 (2002).
- [17] K. Nozari, N. Behrouz, A. Sheykhi, Int. J. Theor. Phys. **52**, 2351 (2013).
- [18] J. Dutta, S. Chakraborty, M. Ansari, Mod. Phys. Lett. A **25**, 3069 (2010);
 D. Jibitesh et al. Int. J. Theor. Phys. **50**, 2383 (2011);
 S. Ghaffari, et al. Phys. Rev. D **91**, 023007 (2015);
 H. Farajollahi, et al. Astrophys. Space Sci. **348**, 253 (2013);
 Sh. Rani, A. Jawad, Int. J. Mod. Phys. D **25**, 1650102 (2016);
 Y. Aguilera, A. Avelino, N. Cruz, S. Lepe, F. Pena, Eur. Phys. J. C **74**, 3172 (2014);
 N. Cruz, S. Lepe, F. Pena, A. Avelino, Eur. Phys. J. C **72**, 2162 (2012);
 S. Ghaffari, M. H. Dehghani, A. Sheykhi, Phys. Rev. D **89**, 123009 (2014);
 A. Jawad, Astrophys Space Sci **360**, 52 (2015);
 A. Jawad, et al. Eur. Phys. J. Plus **131**, 236 (2016);
 A. Jawad, Ines G. Salako, Eur. Phys. J. Plus **130**, 198 (2015).
- [19] X. Wu, R.G. Cai, Z.H. Zhu, Phys. Rev. D **77**, 043502 (2008).
- [20] K. Koyama, Gen. Relativ. Gravit. **40**, 421 (2008);
 M. Li, X. Li, S. Wang and Y. Wang, Commun. Theor. Phys. **56**, 525 (2011) .
- [21] N. Ohta, Phys. Lett. B **695**, 41 (2011).
- [22] P. J. E. Peebles and B. Ratra, Rev. Mod. Phys. **75**, 559 (2003).
- [23] V. Sahni, T. D. Saini, A. A. Starobinsky and U. Alam, JETP Lett. **77**, 201 (2003).
- [24] R. Caldwell and E. V. Linder, Phys. Rev. Lett. **95**, 141301 (2005).